Earthquakes and Structures, *Vol. 17, No. 2 (2019) 191-204*
DOI: https://doi.org/10.12989/eas.2019.17.2.191

Effectiveness of non-linear fluid viscous dampers in seismically isolated buildings

Elif Güler[a] and Cenk Alhan*

Department of Civil Engineering, Istanbul University-Cerrahpaşa, 34320 Avcılar, Istanbul, Turkey

(Received December 19, 2018, Revised April 29, 2019, Accepted May 9, 2019)

Abstract. Near-field earthquake records including long-period high-amplitude velocity pulses can cause large isolation system displacements leading to buckling or rupture of isolators. In such cases, providing supplemental damping in the isolation system has been proposed as a solution. However, it is known that linear viscous dampers can reduce base displacements in case of near-field earthquakes but at the potential expense of increased superstructure response in case of far-field earthquakes. But can non-linear dampers with different levels of non-linearity offer a superior seismic performance? In order to answer this question, the effectiveness of non-linear viscous dampers in reducing isolator displacements and its effects on the superstructure response are investigated. A comparison with linear viscous dampers via time history analysis is done using a base-isolated benchmark building model under historical near-field and far-field earthquake records for a wide range of different levels of non-linearity and supplemental damping. The results show that the non-linearity level and the amount of supplemental damping play important roles in reducing base displacements effectively. Although use of non-linear supplemental dampers may cause superstructure response amplification in case of far-field earthquakes, this negative effect may be avoided or even reduced by using appropriate combinations of non-linearity level and supplemental damping.

Keywords: seismic isolation; non-linear supplemental dampers; viscous dampers; near-field earthquakes

1. Introduction

Seismic isolation offers the protection of both the structural integrity and the contents of a structure simultaneously from harmful effects of ground excitation induced vibrations (Deringöl and Bilgin 2018). The effective earthquake forces and hence the floor accelerations of the structures are reduced by placing the structure on a laterally flexible seismic isolation system. Since a great portion of the relative displacements occur in the seismic isolation system, the superstructure essentially acts like a rigid block which leads to reduced inter-story drift ratios (Komodromos 2000, Warn and Ryan 2012). As of today, seismic isolation is a well-established earthquake resistant design method and thus it is possible to see many practical applications of it worldwide. As an earlier example, within the scope of the replacement project of the San Bernardino County Medical Center, Asher *et al*. (1996) presented the seismic isolation system design of a building whose base isolation system was composed of both high damping rubber bearings and supplemental viscous damping devices. Later, Uçkan *et al*. (2007) reported the applications of seismic isolation to important structures in Turkey including Atatürk Airport Terminal Building, Egegaz LNG Storage Tanks, Bolu Viaducts, Kocaeli University Hospital and Tarabya Hotel. Recently, Cardone and Gesualdi (2014) presented the stages of the seismic rehabilitation process of an existing high-rise reinforced concrete building located in southern Italy through seismic isolation. Sorace *et al*. (2016) performed the finite element analysis of a semicircular marble column and an equestrian bronze sculpture located in the Opificio delle Pietre Dure Institute in Florence and suggested that the main hall be retrofitted via floor-isolation consisting of double curved surface sliders. In parallel with these practical applications, analytical and experimental research studies are still in progress (e.g., Colombo and Almazán 2017, Mazza and Mazza 2017, Moeindarbari and Taghikhany 2018).

Among the challenges that seismic isolation face, the near-field earthquake problem seems to be the hottest that attracts many researchers' attention in the last two decades (e.g., Losanno *et al*. 2017, Mazza *et al*. 2017). This potential problem was first addressed by Hall *et al*. (1995) and Heaton *et al*. (1995). After the 1994 Northridge Earthquake occurred beneath a heavily urbanized area, Hall *et al*. (1995), Heaton *et al*. (1995) emphasized that it may be necessary to develop design codes by noting the potentially destructive effect of the near-source earthquakes. They investigated the seismic performances of the flexible structures (a 20-story steel-frame building and a 3-story base-isolated building) which are vulnerable to near-source ground pulses under the simulated M_w 7.0 earthquake on a blind thrust fault. Later, Alhan and Altun (2009) numerically demonstrated that under the near-field earthquake records including long-period high-amplitude velocity pulses, excessive isolator displacements may come into scene and showed the success of the Uniform Building

*Corresponding author, Professor
E-mail: cenkalhan@istanbul.edu.tr
[a]Ph.D. Student
E-mail: guler.elif@gmail.com

http://www.techno-press.com/journals/eas&subpage=7
ISSN: 2092-7614 (Print), 2092-7622 (Online)

Code (UBC97) in predicting design isolator displacements under near-field earthquake effects via non-linear time history analyses of a 4-story seismically isolated benchmark building. Jensen and Kusanovic (2014) assessed the seismic responses of seismically isolated buildings under the excitations developed by a non-stationary stochastic process with uncertain model parameters and reported that near-field excitations can have significant effects on the reliability-based performance and design of base-isolated buildings. Tajammolian *et al*. (2014) evaluated the impacts of peak ground velocity of near-field pulses on the seismic responses of the base-isolated structures equipped with single friction pendulum, double concave friction pendulum, and triple concave friction pendulum bearings under the near-field ground motions with both fling-step and forward directivity pulses. Alhan *et al*. (2016) emphasized that in case of near-field ground motions, large isolator displacements may cause stiffening of high damping rubber bearings (HDRBs) by comparing seismic responses of six-story base-isolated buildings equipped with high damping rubber bearings considering both non-stiffening and stiffening models under historical and synthetic near-field ground motions. Saifullah and Alhan (2017) demonstrated the necessity of near-source factors specified in the 1997 Uniform Building Code (UBC97) by conducting time history analyses of seismically isolated buildings under a large set of historical earthquakes.

As discussed above, large base displacements in case of near-field earthquakes is a substantial problem that needs to be addressed. Providing supplemental damping in the isolation system has been proposed as a solution for this problem. Hall and Ryan (2000) investigated a six-story base-isolated building designed according to the provisions of 1997 Uniform Building Code (UBC97) and showed that under two most severe simulated ground motion records used in the study, the superstructure may present non-linear behavior due to high (5%) inter-story drift ratios which were shown to be reduced drastically (to 1.3%) via use of supplemental damping with a 20% damping ratio. Sorace and Terenzi (2001a) proposed a non-linear dynamic design procedure for fluid viscous spring-dampers used in base isolation system of building structures. They examined a simple building with a very stiff superstructure and showed that its highest performance is attained starting from rather moderate damping coefficient values. In an accompanying study, in order to show that the non-linear dynamic procedure proposed in Sorace and Terenzi (2001a) can be a viable design approach, Sorace and Terenzi (2001b) applied the subject procedure to two case studies, represented by a reinforced concrete and a steel five-storey frame building with identical global dimensions. Providakis (2008) proposed adding supplemental viscous dampers to the isolation systems of seismically isolated reinforced concrete buildings that consist of lead-rubber bearings in order to avoid large isolator displacements that may occur under near-field excitations. Providakis (2008) also showed that the supplemental viscous damping included in the isolation system against near-field earthquakes may provoke increases in the superstructure responses under moderate strong ground motions coming from far-field sites. Mazza and Vulcano (2009) investigated the effects of supplemental damping at the level of isolation system through numerical analyses and showed that isolator sizes may be reduced by means of supplemental viscous dampers as they reduce isolation system displacement demand. Providakis (2009) showed that providing supplemental damping for both lead-rubber bearings and friction-pendulum system bearings reduces base displacements under near-field earthquake ground motions but may increase the superstructure responses consisting of inter-story drifts and absolute floor accelerations under far-field earthquake ground motions. Despite aforesaid potential disadvantages relating to the increased superstructure responses, passive dampers are still preferred over active or semi-active dampers in practical applications since they require less complicated technology. Applications of the structures with passive dampers are increasing more each year (Martelli and Forni 2011). Important examples of structures protected by means of passive dampers included in the isolation system in different regions of the world include the first seismically isolated high-rise building in Tokyo, Japan protected by 30 low damping rubber bearings and 99 elastic-plastic dampers, the 91 m tall 20-storey steel building of the Suzukakedai Campus of Tokyo Institute of Technology, protected by 16 rubber bearings, 58 steel or oil dampers, and mega X-shape braces, a 5-storey steel and mixed steel-concrete system structure in Japan, with a height of 24.23 m and a total floor area of about 27000 m^2, which was built on lead rubber bearings and viscous and oil dampers, the Chinese stadium protected by rubber bearings and viscous dampers, the National Drama Theatre at Gorno-Altaisk in the Russian Federation retrofitted with high damping rubber bearings and visco-elastic dampers, and Marquam Bridge in Oregon, US retrofitted by means of rubber bearings and elastic-plastic dampers (Martelli 2007, Martelli and Forni 2010, Martelli *et al*. 2012, Martelli *et al*. 2014). One of the most significant actual application of mixed viscous dissipative-base isolation strategy is the Headquarters of the Association Fratellanze Popolare in Florence, Italy which is isolated by means of sliding devices and viscous dampers. Detailed information about the seismic protection of this structure is presented by Sorace and Terenzi (2008).

As discussed above, evidently linear viscous dampers can reduce base displacements in case of near-field earthquakes but at the potential expense of increased superstructure response in case of far-field earthquakes. And the question is: Can non-linear dampers offer a superior seismic performance? Regarding the answer, the comparative evaluation of the seismic performance of linear and non-linear viscous dampers has not been sufficiently addressed by researchers. An initial attempt regarding this topic was provided by Tsopelas *et al*. (1994). Tsopelas *et al*. (1994) demonstrated the capability of non-linear viscous fluid dampers in dissipating more energy per cycle under harmonic motion. Research studies on the preference of linear or non-linear dampers have begun considering the need to limit the base displacements and the preference of passive dampers (Goel 2005, Wolff *et al*. 2015, Saha *et al*. 2018). Goel (2005) compared the seismic response of one-story structural systems with non-linear fluid viscous dampers with respect to those with equivalent linear dampers under harmonic and earthquake loadings in order to investigate the influence of damper non-linearity on the effects of plan asymmetry. Saha *et al*. (2018) investigated the optimum performance of a passive seismic isolation system equipped with linear or non-linear fluid viscous dampers in the context of a benchmark *bridge* using six earthquake records. They assessed the influence of the velocity exponent and concluded that non-linear viscous dampers were more effective in reducing the bridge response. And recently Wolff *et al*. (2015) experimentally investigated the effect of linear and non-linear viscous damping devices on the behavior of the seismically isolated frames with low damping elastomeric and single friction pendulum bearings. However, they only used a single type of non-linear damper with a non-linearity exponent and a supplemental damping coefficient for a specific design. In order to contribute to the research in this area, we parametrically investigate the effectiveness of non-linear viscous dampers in reducing isolator displacements and its effects on the superstructure response including structural base shear, floor accelerations and story drift ratios in comparison with linear viscous dampers via time history analysis of a benchmark multi-story three-dimensional base-isolated building model for a wide range of different non-linearity exponents (i.e., different levels of non-linearity) and for a range of different supplemental viscous damping coefficients (i.e., damping ratios). For this purpose, 3D-BASIS-ME (Tsopelas *et al*. 1994), an improved version of 3D-BASIS (Nagarajaiah *et al*. 1991) software developed to conduct earthquake analyses of seismically isolated buildings, is used to model the six-story benchmark seismically isolated buildings equipped with non-linear or linear viscous dampers placed in the seismic isolation system in parallel with rubber isolators. The parameters that are taken into account include two isolation periods (i.e., 3 s and 5 s), four levels of supplemental damping ratios (i.e., 10%, 20%, 30%, and 40%), a no supplemental damping case, and four levels of supplemental viscous damping non-linearity coefficients. Thus, 34 different cases are evaluated under six different historical earthquake records (three near-field and three far-field).

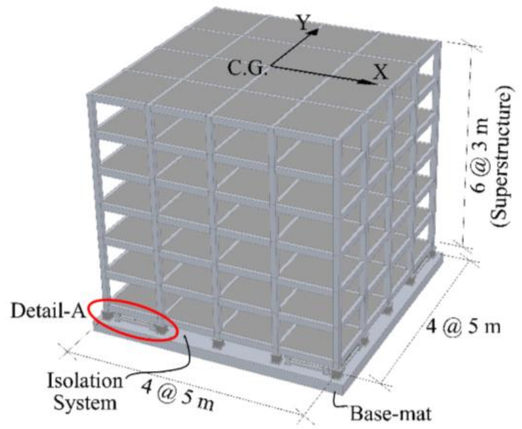

(a) Base-isolated benchmark building

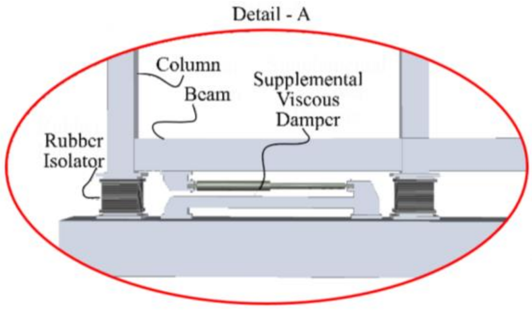

(b) Close-up view of the supplemental fluid viscous damper

Fig. 1 Three dimensional view of the base-isolated benchmark building equipped with supplemental fluid viscous dampers

2. Structural model

In this study, a benchmark six-story base-isolated building equipped with (i) linear viscous dampers (Case A), (ii) non-linear viscous dampers (Case B), and (iii) no supplemental dampers (Case C), is used. It consists of two main parts: the superstructure and the seismic isolation system. The three dimensional view of the base-isolated building that is equipped with supplemental viscous dampers (Case A and B) is given in Fig. 1.

2.1 Superstructure

The superstructure is a six-story reinforced concrete frame (Alhan and Sürmeli 2011). The dimensions of each column and beam elements are 45 cm×45 cm and 30 cm×55 cm, respectively. The modulus of elasticity is 32000 MPa. The total mass of the building including the isolation floor is M=2240 kNs^2/m. All floors are assumed to be rigid diaphragms and each one has three degrees of freedom: X, Y, and rotational. Since the superstructure is assumed to be fully symmetric, there exists no eccentricity. The modal damping ratios and translational periods in each of the main lateral direction are 5% and 0.68 s, respectively. The natural period, eigenvalues and eigenvectors of the superstructure, which are required as input in 3D-BASIS-ME (Tsopelas *et al*. 1994), are obtained from the modal analyses conducted in SAP2000 (2011).

2.2 Seismic isolation system

The seismic isolation system consists of rubber isolators placed underneath each column which are connected with a rigid base floor. In addition, in cases A and B, linear and non-linear supplemental viscous dampers are placed in parallel with the rubber isolators, respectively (Güler 2013). Hysteretic non-linear behavior of the rubber based bearings is defined using smooth bi-linear force-deformation relationship. In order to keep the isolation systems as generic ones, within the scope of this study, isolator behavior is defined by main characteristic parameters that yield target rigid-body-mode isolation periods. The parameters which characterize a non-linear isolation system composed of such bearings are described here (Nagarajaiah *et al*. 1991). In order to take a typical range of seismic isolation systems into account, the rigid-body-mode

Table 1 Characteristics of linear and non-linear supplemental viscous dampers

		T_0=3 s				T_0=5 s			
ζ (%)	α^{*1} (-)	System code	C (kNs/m)	F_{DT}^{*2} (kN)	V_D^{*2} (m/s)	System code	C (kNs/m)	F_{DT}^{*2} (kN)	V_D^{*2} (m/s)
10	0.50	T3Z10A050	1181.75	1360.00	1.325	T5Z10A050	611.95	641.75	1.100
	0.75	T3Z10A075	1059.25	1360.00	1.396	T5Z10A075	588.38	641.75	1.123
	1.00	T3Z10A100	938.29	1360.00	1.450	T5Z10A100	563.00	641.75	1.140
	1.25	T3Z10A125	826.25	1360.00	1.490	T5Z10A125	537.13	641.75	1.153
20	0.50	T3Z20A050	2234.00	2316.50	1.075	T5Z20A050	1175.08	1151.50	0.960
	0.75	T3Z20A075	2075.00	2316.50	1.158	T5Z20A075	1154.63	1151.50	0.996
	1.00	T3Z20A100	1876.58	2316.50	1.234	T5Z20A100	1125.95	1151.50	1.023
	1.25	T3Z20A125	1677.25	2316.50	1.295	T5Z20A125	1092.48	1151.50	1.043
30	0.50	T3Z30A050	3080.00	3037.50	0.973	T5Z30A050	1629.40	1577.50	0.937
	0.75	T3Z30A075	3037.50	3037.50	0.999	T5Z30A075	1673.48	1577.50	0.924
	1.00	T3Z30A100	2815.00	3037.50	1.079	T5Z30A100	1688.92	1577.50	0.934
	1.25	T3Z30A125	2558.95	3037.50	1.147	T5Z30A125	1654.05	1577.50	0.963
40	0.50	T3Z40A050	3772.50	3607.50	0.914	T5Z40A050	2111.50	2002.75	0.900
	0.75	T3Z40A075	3930.00	3607.50	0.892	T5Z40A075	2169.83	2002.75	0.899
	1.00	T3Z40A100	3753.15	3607.50	0.961	T5Z40A100	2251.90	2002.75	0.889
	1.25	T3Z40A125	3468.25	3607.50	1.032	T5Z40A125	2358.63	2002.75	0.877

*1: α=1.00 corresponds to linear viscous dampers - Case A and other α values correspond to non-linear viscous dampers - Case B.

*2: Total damper force (F_{DT}=25×F_D) and damper velocity values (V_D) correspond to velocities under LGP000 earthquake record.

isolation periods (T_0) are assumed as 3 s and 5 s for two main cases. Consequently, the rigid-body-mode angular frequencies (ω_0) are obtained as 2.09 rad/s and 1.26 rad/s using $T_0=2\times\pi/\omega_0$ and the second branch stiffness (K_2) values are calculated as 9825.74 kN/m and 3537.27 kN/m via $\omega_0=(K_2/M)^{½}$ for 3 s and 5 s isolation periods, respectively. The second branch to first branch stiffness ratio (K_2/K_1) is assumed as 0.1, which is a typical design value. So, the first branch stiffness (K_1) values are calculated as 98257.39 kN/m and 35372.66 kN/m for 3 s and 5 s isolation periods, respectively. The first branch limit force (F_y) values are calculated as 982.57 kN and 1061.18 kN using $F_y=K_1\times D_y$ by assuming the first branch limit displacements (D_y) as 10 mm and 30 mm for 3 s and 5 s isolation periods, respectively. Then, the characteristic strength (Q) values corresponding to T_0=3 s and 5 s cases are calculated with K_1-K_2=Q/D_y (Naeim and Kelly 1999) as 884.30 kN and 995.07 kN. Therefore, the characteristic strength ratio (Q/W) values result in 4.02% and 4.35%, which fall in the range of typical characteristic strength ratios used in design of seismically isolated buildings. For a single isolator, second branch stiffness (k_2), first branch stiffness (k_1), first branch limit force (f_y) and characteristic strength (q) values are calculated by dividing the corresponding total values (K_2, K_1, F_y and Q) by the number of isolators i.e., 25.

For the base isolation systems that contain the supplemental viscous dampers in parallel with the rubber isolators (cases A and B), the behavior of the viscous damper is modeled by $F_D=c\times V_D^{\alpha}$ (Tsopelas *et al*. 1994). Here, F_D is the damper force; V_D is the relative velocity across the damper; c is the viscous damping coefficient and α is the velocity exponent. Existing studies in the literature report velocity exponents (i.e., non-linearity coefficients) to take on values from 0.20 to 1.20, depending on the design choice that describes the level of non-linearity (Constantinou and Symans 1992, Goel 2004, Bahnasy and Lavan 2013, Narkhade and Sinha 2014). While velocity exponents vary approximately in the range of 0.50 to 0.80 for moderately non-linear orifice viscous dampers, they are in the range of 0.80 to 1.00 for nearly linear viscous dampers. And also, highly non-linear viscous dampers, operating on an annular flow mechanism of silicone fluids exhibit non-linearity coefficients in the range of 0.10-0.20 (Sorace and Terenzi 2001a, 2008). However, the numerical investigation in this study is limited to α values of 0.50, 0.75, 1.00, and 1.25.

For a linear viscous damper, the velocity exponent value is equal to 1.00. In case of linear viscous dampers, the total viscous damping coefficient (C) is calculated as $C=2\times\zeta\times M\times\omega_0$ where ζ is the supplemental damping ratio which is considered as 10%, 20%, 30%, and 40% in this study. The viscous damping coefficient of a single damper (c) is calculated by dividing the total viscous damping coefficient by the number of dampers. The supplemental viscous damping coefficients of non-linear viscous dampers ($\alpha\neq1.00$) are calculated such that the non-linear viscous damper forces are equal to the linear ones under near-field LGP000 record (see Section 3) which is selected as the target design earthquake that imposes large damper forces. The characteristics of the linear and the non-linear supplemental viscous dampers used in the study are given in Table 1. It should be noted that there also exists inherent damping of isolators and it contributes to the energy balance of the seismic response. However, the level of this contribution varies from earthquake to earthquake as the equivalent linear viscous damping would be dependent on the isolation system displacement (Alhan and Özgür 2015).

Table 2 Characteristics of the earthquake records

	Earthquake	Record date	Component	Station name	*r* (km)	*PGA* (g)	*PGV* (cm/s)
Near-field	Loma Prieta	10/18/1989	LGP000	LGPC	6.1	0.563	94.8
	Northridge	01/17/1994	WPI046	Newhall-W. Pico Canyon Rd.	7.1	0.455	92.8
	Erzincan	03/13/1992	ERZ-NS	Erzincan	2.0	0.515	83.9
Far-field	Northridge	01/17/1994	MUL009	Beverly Hills-Mulhol	19.6	0.416	59.0
	Northridge	01/17/1994	RO3-090	Sun Valley-Roscoe	12.3	0.443	38.2
	Imperial Valley	05/19/1940	I-ELC180	El Centro Array #9	8.3	0.313	29.8

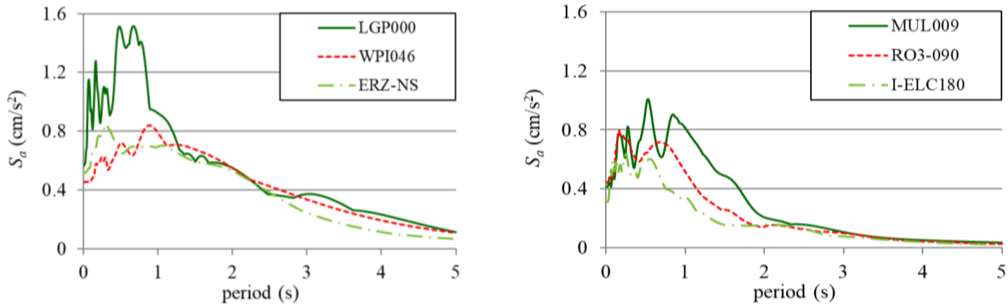

(a) Acceleration response spectra for near-field records (b) Acceleration response spectra for far-field records

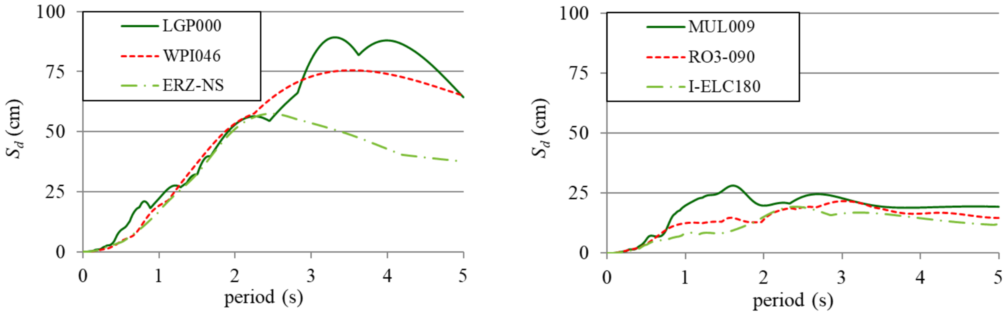

(c) Displacement response spectra for near-field records (d) Displacement response spectra for far-field records

Fig. 2 10% damped acceleration and displacement response spectra

3. Characteristics of the earthquake data

Six historical earthquake records, representatives near-field and far-field earthquakes, are obtained from the ground motion database of the Pacific Earthquake Engineering Research Center (Berkeley 2013). Information on these records is presented in Table 2. In this table, *r* is the closest distance to the fault, *PGA* is the peak ground acceleration, and *PGV* is the peak ground velocity.

Typical near-field earthquake records are characterized by the velocity pulses with long-periods and high-amplitudes (Somerville 1998, Nagarajaiah and Ferrell 1999, Agrawal *et al*. 2002, He and Agrawal 2008). Additionally, near-field earthquake effects typically occur in the records which are nearby locations, say within the 15 km of the epicenter (Hoseini Vaez *et al*. 2014). While velocity pulses can visually be classified, recent efficient algorithm proposed by Shahi and Baker (2014) based on wavelet analysis that identifies and extracts the pulses at arbitrary orientations in multicomponent ground motions can also be used for a more precise classification. A comparative evaluation of different algorithms for detecting pulses based on wavelet analysis can be found in Mazza (2018). On the other hand, typical earthquake records with high-frequencies are far-field earthquake records which are recorded at distant points to the epicenter. In this study, LGP000 component of the Loma Prieta earthquake, WPI046 component of the Northridge earthquake and ERZ-NS component of the Erzincan earthquake are considered as representatives of pulse-like near-field earthquakes with high peak ground velocities (83.9 cm/s~94.8 cm/s) occurring at closest fault distances of r<10 km. MUL009 component of the Northridge earthquake, RO3-090 component of the Northridge earthquake and I-ELC180 component of the Imperial Valley earthquake have lower peak ground velocities (29.8 cm/s~59.0 cm/s) with no pulses. These records are used in this study as representatives of far-field earthquakes.

The 10% damped acceleration and displacement response spectra for the earthquake records used in this study are given in Fig. 2. It should be noted that for the period range corresponding to the isolation periods (T_0≥3 s), the near-field records result in much larger spectral displacements compared to far-field records. Such large displacements are the reason for the potential need for supplemental dampers. Due to economical and safety concerns, it may be preferable to reduce such large displacements by using linear or non-linear viscous

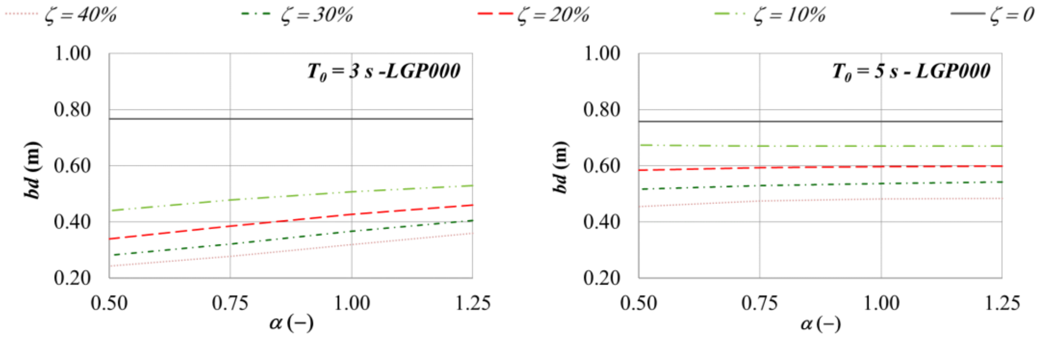

(a) For the near-field LGP000 record and T_0=3 s (b) For the near-field LGP000 record and T_0=5 s

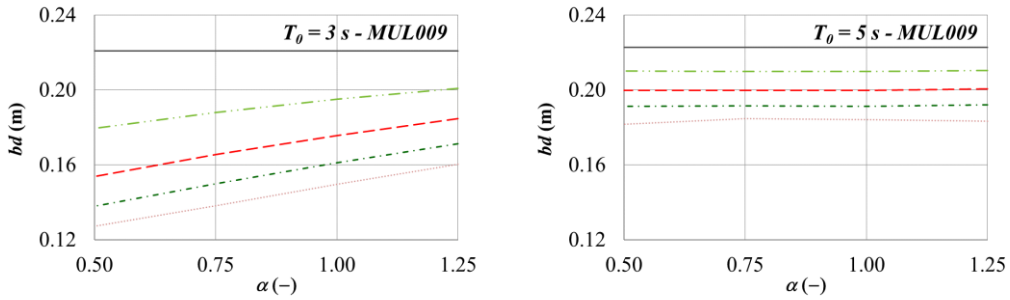

(c) For the far-field MUL009 record and T_0=3 s (d) For the far-field MUL009 record and T_0=5 s

Fig. 3 Peak base displacements (*bd*)

dampers in the seismic isolation system. But once the supplemental dampers are placed in the seismic isolation system as a measure against near-field records, they will be there when more frequent far-field records hit. So, in this study, the damper characteristics are selected (see Table 1) using the largest near-field record, i.e., LGP000, and then the seismic performance of the building is evaluated for other similar near-field and also other typical far-field earthquake records (see Table 2 and Fig. 2).

4. Discussion of seismic analyses results

Structural response parameters including base displacement, superstructure base shear, floor accelerations and inter-story drift ratios are obtained via non-linear time history analyses under three near-field earthquake records (LGP000, WPI046 and ERZ-NS) and three far-field earthquake records (MUL009, RO3-090 and I-ELC180) for the benchmark six-story base-isolated building equipped with (i) linear viscous dampers, (ii) non-linear viscous dampers, and (iii) no supplemental dampers. The amounts of the supplemental damping ratios are considered as ζ=10%, 20%, 30%, and 40%. Two different isolation system periods are taken into account: T_0=3 s and 5 s. The superstructure is assumed to remain linear elastic doing the analyses. Soil-structure interaction and vertical earthquake excitation are not considered.

4.1 Isolation system response

Peak base displacement responses of the seismically isolated buildings with no supplemental dampers are presented in Table 3. Base displacement responses typically

Table 3 Peak base displacements with no supplemental dampers

Isolation period	Peak base displacement (cm)					
	Near-field records			Far-field records		
	LGP000	WPI046	ERZ-NS	MUL009	RO3-090	I-ELC180
T_0=3 s	76.69	72.66	61.06	22.10	12.85	8.56
T_0=5 s	75.85	82.54	56.09	22.27	15.05	12.74

are much higher under the near-field records compared to the far-field ones, which is compatible with the spectral displacement values given in Fig. 2. While peak base displacement response under the near-field records vary between the 56.09 cm (ERZ-NS) and 82.54 cm (WPI046), even the maximum value under the far-field earthquake records is observed to be much less, i.e., 22.27 cm (MUL009).

Evidently, the near-field earthquake records containing velocity pulses with long-periods and high-amplitudes result in large base displacements. These large base displacements may cause both rupture and/or buckling of the isolators and economic problems by damaging the content and/or production process (Hall *et al*. 1995, Heaton *et al*. 1995, Alhan and Altun 2009, Jensen and Kusanovic 2014, Tajammolian *et al*. 2014, Alhan *et al*. 2016, Saifullah and Alhan 2017). Thus, while it may be unnecessary in case the structure is subjected to far-field earthquakes, the use of supplemental damping against near-field earthquakes in order to reduce such large base displacements may be available solution. However, following question still stands: Are linear dampers or non-linear dampers more effective in limiting base displacements?

Fig. 3 presents the peak base displacements (*bd*) under the LGP000 representing near-field records and the

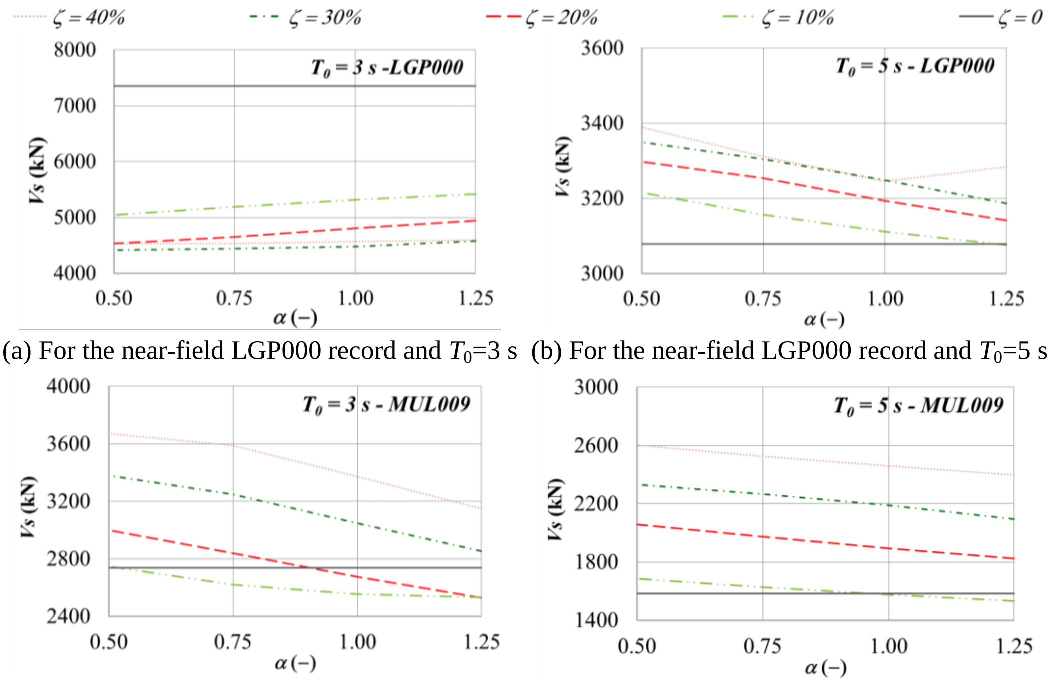

(a) For the near-field LGP000 record and T_0=3 s (b) For the near-field LGP000 record and T_0=5 s

(c) For the far-field MUL009 record and T_0=3 s (d) For the far-field MUL009 record and T_0=5 s

Fig. 4 Peak superstructure base shear forces (*Vs*)

MUL009 representing far-field records for T_0=3 s and 5 s isolation periods. The amounts of the supplemental damping ratios (ζ) are taken into account as 10%, 20%, 30%, and 40%. And also no supplemental damper case (ζ=0%) is shown with a solid line. On the other hand, non-linearity exponents (α) are considered as 0.50, 0.75, 1.00, and 1.25 where α=1.00 represents the linear case. As seen in Fig. 3, supplemental dampers significantly reduce the peak base displacements with respect to no supplemental damper case and increasing damping ratios monotonically decrease the peak base displacements for both linear and non-linear cases. Effect of the use of supplemental linear dampers, only was investigated by Providakis (2008, 2009) in terms of peak base displacements who reached similar findings. It is observed from Fig. 3 that non-linearity of the supplemental dampers may play an important role in reducing base displacements further, the level of which depends on the isolation system and earthquake record characteristics. Furthermore, it is observed that the non-linearity exponent may also effect the amount of the reduction of base displacement with respect to no supplemental damper case of the cases presented in Fig. 3, smaller non-linearity exponents result in much smaller peak base displacements for T_0=3 s isolation systems (see Fig. 3(a) and 3(c)). Please note that the average tendencies of the above-discussed issues are presented later in Section 4.3 such that all earthquake records given in Table 2 are taken into account.

4.2 Superstructure response

Fig. 4 presents the peak superstructure base shear forces (*Vs*) under the near-field LGP000 and far-field MUL009 records for T_0=3 s and 5 s isolation periods and for ζ=10%, 20%, 30%, and 40% supplemental damping ratios. And also no supplemental damper case (ζ=0%) is shown with a solid line. Non-linearity exponents (α) considered are 0.50, 0.75, 1.00, and 1.25 where α=1.00 represents the linear case.

As seen in Fig. 4(c) and 4(d), an amplification in the superstructure base shear force comes into scene as a result of using supplemental damping, either linear or non-linear, under far-field earthquakes. The amount of amplification continues to increase as supplemental damping ratio (ζ) is further increased. In addition, smaller non-linearity exponent (α) (which was beneficial in terms of base displacement response) unfortunately causes higher superstructure base shear forces. On the other hand, although a similar behavior may be observed (see Fig. 4(b)), there may be a reverse behavior where higher supplemental damping ratio and smaller non-linearity exponent result in smaller superstructure base shear force (Fig. 4(a)) under near-field earthquakes.

In the previous section (Section 4.1), it is revealed that use of supplemental damping, in particular non-linear dampers with small non-linearity exponents, may serve better in reducing base displacements compared to linear ones. However, evaluating the influence of using non-linear supplemental dampers with high damping ratios on the superstructure response is also necessary. In this context, answering the following question is also important: May using supplemental damping worsen the superstructure response in case of far-field records? It should be noted that although this phenomenon has been studied for linear dampers before (Hall and Ryan 2000, Providakis 2008, Mazza and Vulcano 2009, Providakis 2009) but it is yet to be examined for non-linear dampers.

The peak total floor accelerations (*a*) are presented in Figs. 5 and 6 for T_0=3 s and 5 s isolation periods,

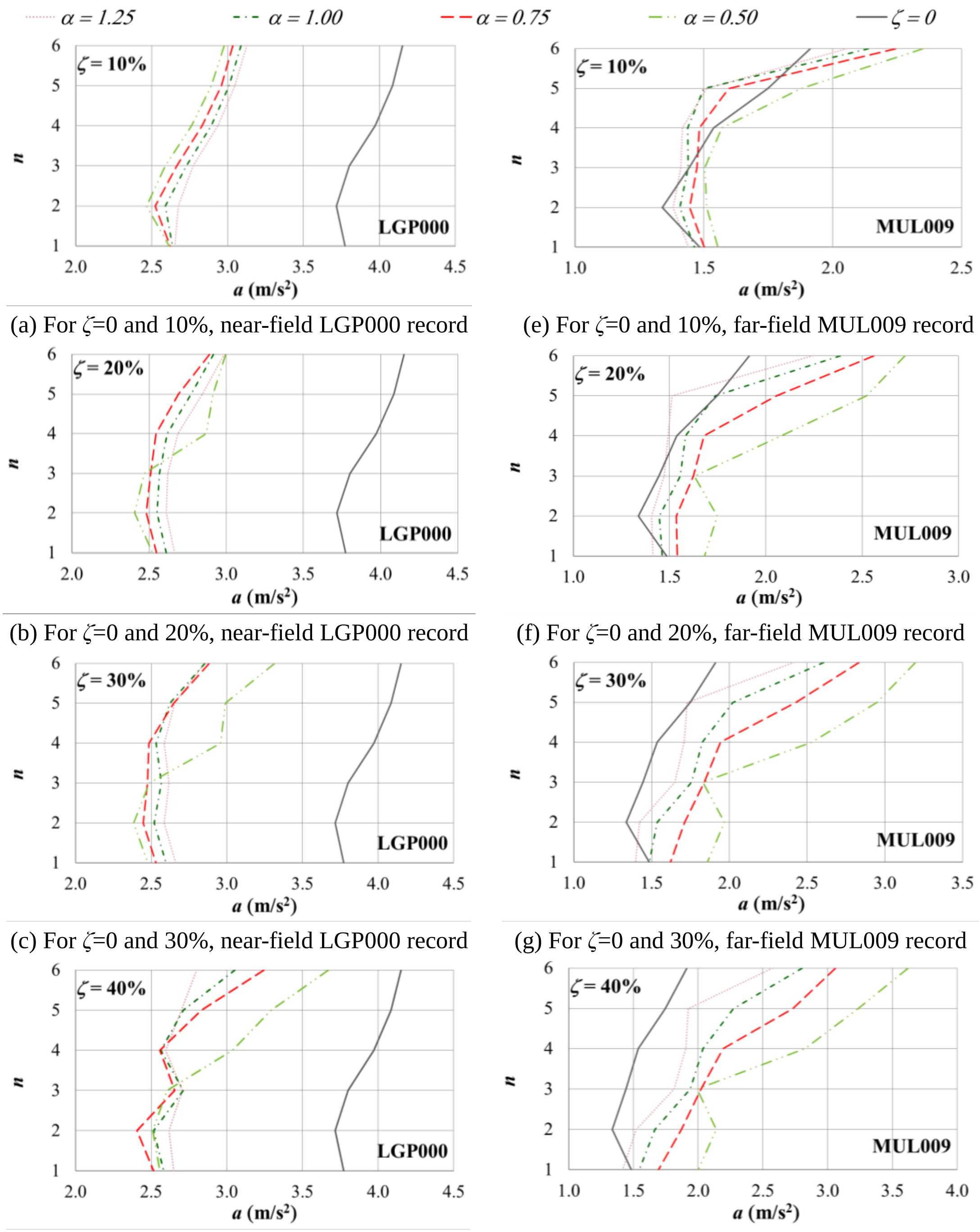

(a) For ζ=0 and 10%, near-field LGP000 record

(e) For ζ=0 and 10%, far-field MUL009 record

(b) For ζ=0 and 20%, near-field LGP000 record

(f) For ζ=0 and 20%, far-field MUL009 record

(c) For ζ=0 and 30%, near-field LGP000 record

(g) For ζ=0 and 30%, far-field MUL009 record

(d) For ζ=0 and 40%, near-field LGP000 record

(h) For ζ=0 and 40%, far-field MUL009 record

Fig. 5 Peak total floor accelerations (a) for T_0=3 s

respectively and the peak inter-story drift ratios (Δ) are presented in Figs. 7 and 8 for T_0=3 s and 5 s isolation periods, respectively. For visual convenience, no supplemental damper case (ζ=0%) is shown with a solid line, while in plots provided for ζ=10%, 20%, 30%, and 40% cases, separately. In these plots, α=0.50, 0.75, 1.00, and 1.25 non-linearity exponent cases are shown with dashed or dotted lines where α=1.00 represents the linear case. Here, LGP000 and MUL009 earthquake records are presented as representatives of the near-field and far-field earthquake records, respectively. Since the peak total floor accelerations and the peak inter-story drift ratios show alterations depending on the story level, profiles are given for all story levels.

As will be discussed next, the general tendencies observed in terms of total floor accelerations and inter-story drift ratios are similar to each other which both are also similar to the general tendencies observed in terms of superstructure base shear. Figs. 5(e)-(h) and Figs. 6(e)-(h) show that use of supplemental damping, whether linear or non-linear, and further increasing supplemental damping ratio typically increases floor accelerations under far-field earthquakes. Similarly, smaller non-linearity exponent also typically results in higher floor accelerations for far-field

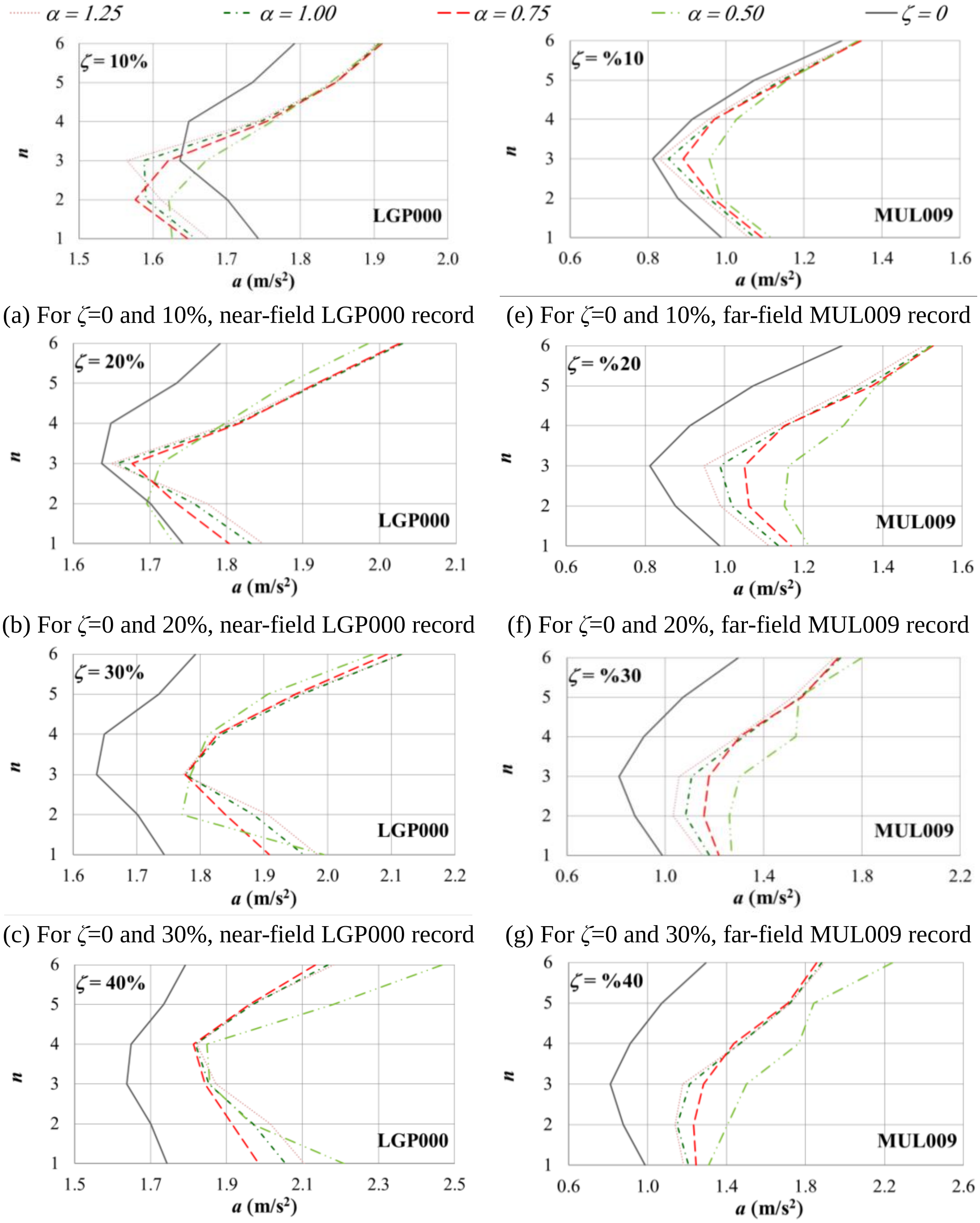

(a) For ζ=0 and 10%, near-field LGP000 record (e) For ζ=0 and 10%, far-field MUL009 record

(b) For ζ=0 and 20%, near-field LGP000 record (f) For ζ=0 and 20%, far-field MUL009 record

(c) For ζ=0 and 30%, near-field LGP000 record (g) For ζ=0 and 30%, far-field MUL009 record

(d) For ζ=0 and 40%, near-field LGP000 record (h) For ζ=0 and 40%, far-field MUL009 record

Fig. 6 Peak total floor accelerations (a) for T_0=5 s

earthquakes. The severity of the aforementioned amplification changes from floor to floor. Similar behavior can be observed in terms of inter-story drift ratios (see Figs. 7(e)-(h) and Figs. 8(e)-(h)). On the other hand, although increased supplemental damping may increase floor accelerations Figs. 6(a)-(d) just like it is observed for far-field earthquakes it may also decrease (Figs. 5(a)-(d)) floor accelerations. Similar observations hold true for inter-story drift ratios (Figs. 7(a)-(d), Figs. 8(a)-(d)).

4.3 Ratios of supplemental-damping to no-supplemental-damping responses - a comparative evaluation

In order to quantify the efficiency of non-linear supplemental damping with respect to the linear supplemental damping and no supplemental damping cases, the response ratios are obtained by dividing the peak response values of supplemental damping cases to those of no supplemental damping case. In this context, in order to obtain the average tendencies of the peak response ratios, for near-field records (LGP000, WPI046 and ERZ-NS), the mean values of the ratios of peak structural responses including peak base displacements (rd), peak superstructure base shear forces (rVs), peak top floor accelerations (ra) and peak roof drift ratios ($r\Delta$) are presented in Fig. 9(a) and 9(b) for T_0=3 s and 5 s isolation periods, respectively. And

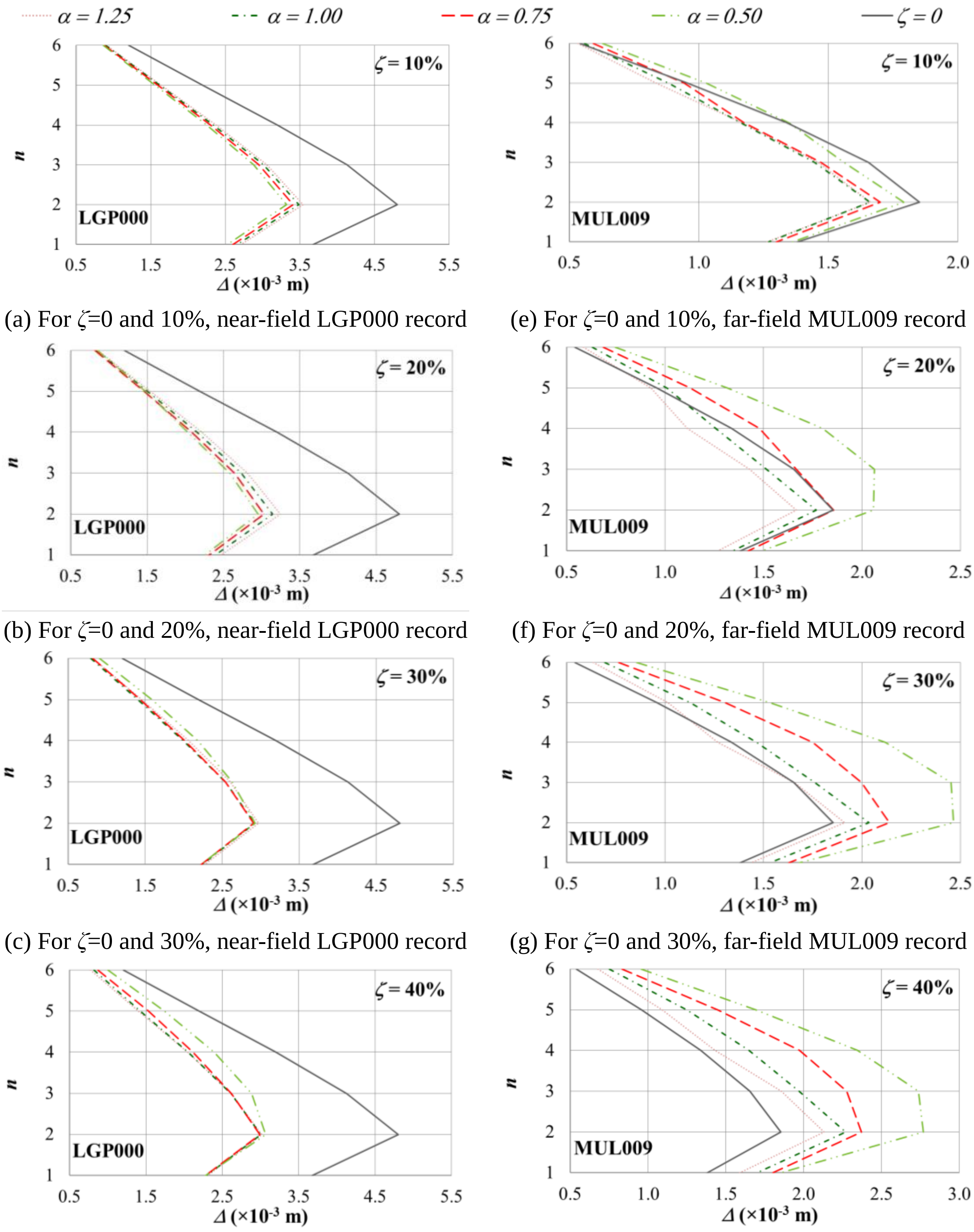

(a) For ζ=0 and 10%, near-field LGP000 record (e) For ζ=0 and 10%, far-field MUL009 record

(b) For ζ=0 and 20%, near-field LGP000 record (f) For ζ=0 and 20%, far-field MUL009 record

(c) For ζ=0 and 30%, near-field LGP000 record (g) For ζ=0 and 30%, far-field MUL009 record

(d) For ζ=0 and 40%, near-field LGP000 record (h) For ζ=0 and 40%, far-field MUL009 record

Fig. 7 Peak inter-story drift ratios (Δ) for T_0=3 s

similarly, Fig. 9(c) and 9(d) present the mean values of ratios of peak structural responses for far-field records (MUL009, RO3-090 and I-ELC180) for T_0=3 s and 5 s isolation periods, respectively. Since the peak total floor accelerations and the peak inter-story drift ratios vary from floor to floor, peak top floor accelerations and peak roof drift ratios are considered in this section. Please note that the roof drift ratios are obtained by dividing the maximum relative displacement (on the top floor) with respect to the base to the building height, h=18 m. Here, the amounts of the supplemental damping ratios (ζ) are taken into account as 10%, 20%, 30%, and 40% and non-linearity exponents (α) are considered as 0.50, 0.75, 1.00, and 1.25 where α=1.00 represents the linear case. Please note that in Fig. 9 if mean values of the responses take values smaller than 1.00, it means that providing linear or non-linear supplemental dampers enhance the seismic performance by reducing the responses with respect to the no damper case.

As seen in Fig. 9, supplemental dampers significantly reduce the peak base displacements with respect to no supplemental damper case and increasing damping ratios monotonically decrease the peak base displacements for both linear and non-linear cases. And also, it is observed from Fig. 9 that the non-linearity levels of the supplemental

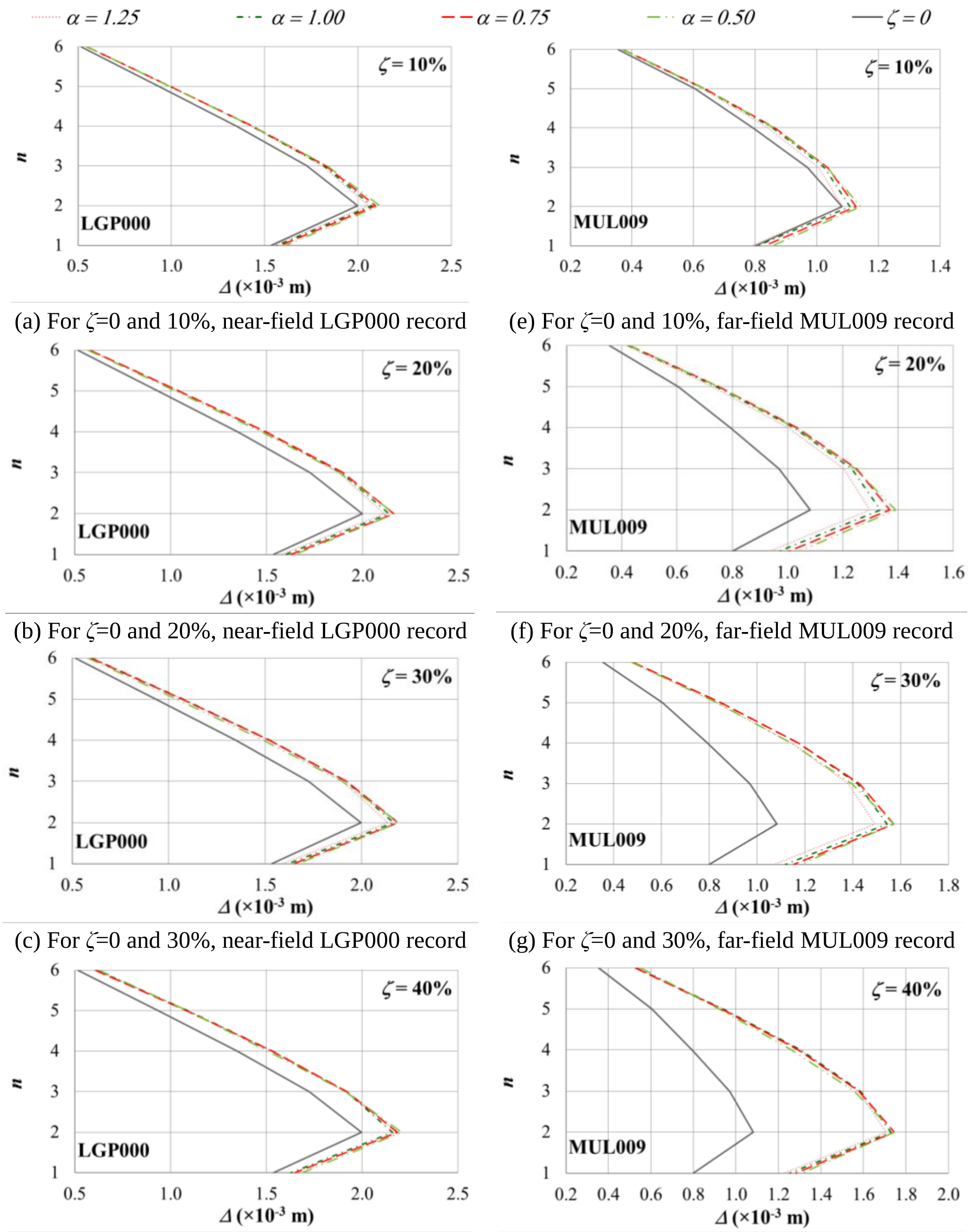

(a) For ζ=0 and 10%, near-field LGP000 record

(e) For ζ=0 and 10%, far-field MUL009 record

(b) For ζ=0 and 20%, near-field LGP000 record

(f) For ζ=0 and 20%, far-field MUL009 record

(c) For ζ=0 and 30%, near-field LGP000 record

(g) For ζ=0 and 30%, far-field MUL009 record

(d) For ζ=0 and 40%, near-field LGP000 record

(h) For ζ=0 and 40%, far-field MUL009 record

Fig. 8 Peak inter-story drift ratios (Δ) for T_0=5 s

dampers may play important role in reducing base displacements (Figs. 9(a)-(d)). Particularly, in case of near-field earthquakes where large base displacements become an issue, it is seen that use of smaller non-linearity exponents may help decreasing peak base displacements further (Fig. 9(a)).

The general tendencies observed in terms of superstructure responses (base shear, peak top floor accelerations and peak roof drift ratios) are similar to each other. Fig. 9(c) and 9(d) show that use of supplemental damping, whether linear or non-linear, and further increasing supplemental damping ratio typically increases peak superstructure base shear, peak top floor accelerations and peak roof drift ratios under far-field earthquakes. In addition, smaller non-linearity exponent also typically results in higher superstructure responses for far-field earthquakes. For near-field earthquakes, higher supplemental damping and smaller non-linearity exponent may decrease (see Fig. 9(a)) or increase (see Fig. 9(b)) the peak superstructure response ratios.

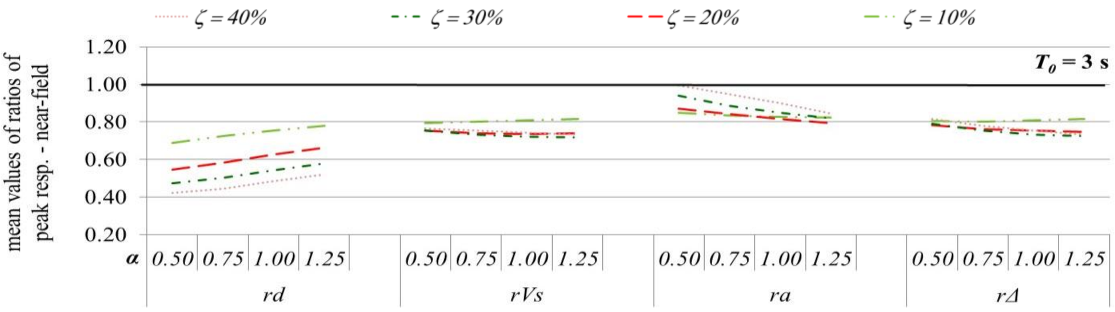

(a) For near-field records and T_0=3 s

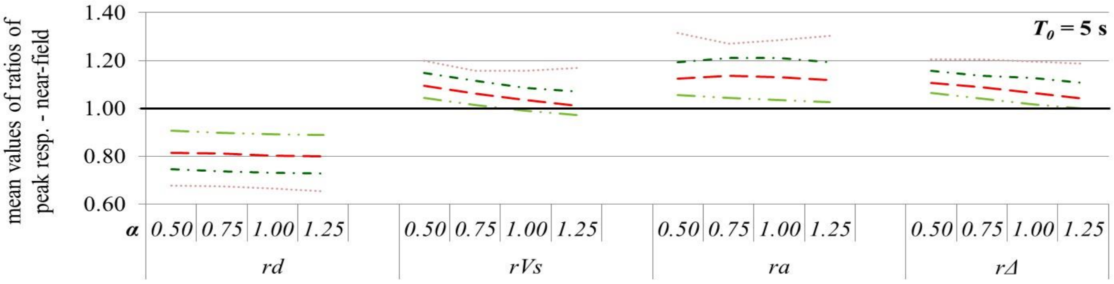

(b) For near-field records and T_0=5 s

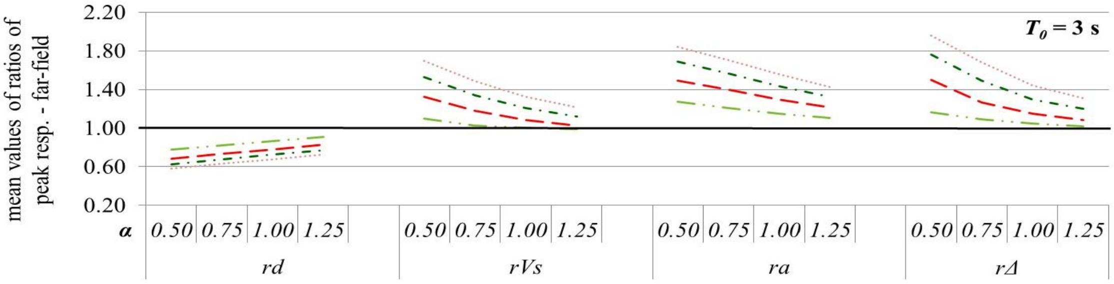

(c) For far-field records and T_0=3 s

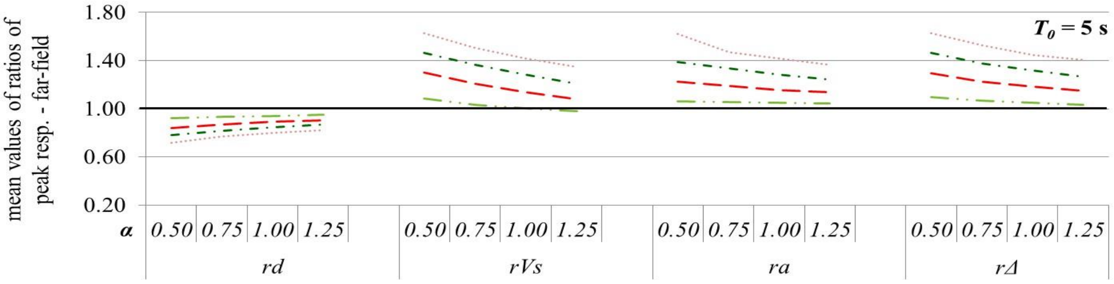

(d) For far-field records and T_0=5 s

Fig. 9 Mean values of ratios of peak structural responses including base displacement (*rd*), superstructure base shear forces (*rVs*), top floor accelerations (*ra*) and roof drift ratios (*rΔ*)

5. Conclusions

In this paper, the effectiveness of non-linear viscous dampers in reducing isolator displacements and its effects on the superstructure response including structural base shear, floor accelerations and story drift ratios are parametrically investigated in comparison with linear viscous dampers. For this purpose, time history analyses of a benchmark base-isolated building model are conducted under near-field and far-field earthquakes. The parameters that are taken into account include two different isolation periods (i.e., T_0=3 s and 5 s), four different levels of supplemental damping ratios (i.e., ζ=10%, 20%, 30%, and 40%) and also no supplemental damping case (ζ=0%), and four different levels of supplemental viscous damping non-linearity coefficients (α=0.50, 0.75, 1.00 and 1.25 where α=1.00 represents the linear case). Based on the results of the analyses conducted here, following conclusions are reached:

- Use of supplemental viscous damping significantly reduces the peak base displacement response with respect to no supplemental damping case and increasing supplemental damping ratios monotonically decreases the peak base displacement responses for both linear and non-linear damping cases.
- Non-linearity level of the supplemental dampers may play an important role in reducing base displacements: the smaller non-linearity exponents may help achieving

smaller peak base displacements, which would be particularly useful in case of near-field earthquakes.

• Amplification in the peak superstructure responses including superstructure base shear force, peak total floor accelerations and peak inter-story drift ratios may come into scene as a result of using supplemental damping, either linear or non-linear in case of *far-field earthquake records*. The amount of amplification steadily increases as supplemental damping ratio (ζ) is further increased and non-linearity exponent (α) is decreased. For *near-field earthquake records*, use of higher supplemental damping ratio and smaller non-linearity exponent may increase but also may decrease superstructure responses depending on the earthquake record.

• Effect of the non-linearity level on the structural responses and thus the effectiveness of non-linear fluid viscous dampers in seismically isolated buildings vary depending on the structural response type, isolation system characteristics, supplemental damping ratio and earthquake record characteristics. Desired seismic performance could be obtained with an appropriate combination of the supplemental damping ratio and the non-linearity exponent.

It should be noted here that the conclusions reached above are based on a limited number of ground motions (i.e. six earthquakes). Thus, further studies need to be carried out using more ground motions as part of the future work before any firm conclusions can be drawn.

Acknowledgments

This work was supported by the Scientific Research Projects Coordination Unit of Istanbul University. Project No: BAP-19354.

References

Agrawal, A.K., He, W.L. and Yang, J.N. (2002), "Performance evaluation of semi-active control systems for a benchmark cable-stayed bridge", *Proceedings of the 7th U.S. National Conference on Earthquake Engineering*, Boston, MA, July.

Alhan, C. and Altun, M. (2009), "Performance of non-linear base isolation systems designed according to uniform building code", *Proceedings of the 5th International Advanced Technologies Symposium*, Karabuk, Turkey, May.

Alhan, C. and Özgür, M. (2015), "Seismic responses of base-isolated buildings: efficacy of equivalent linear modeling under near-fault earthquakes", *Smart Struct. Syst.*, **15**(6), 1439-1461. https://doi.org/10.12989/sss.2015.15.6.1439.

Alhan, C. and Sürmeli, M. (2011), "Shear building representations of seismically isolated buildings", *Bull. Earthq. Eng.*, **9**(1643), 1643-1671. https://doi.org/10.1007/s10518-011-9293-z.

Alhan, C., Gazi, H. and Kurtuluş, H. (2016), "Significance of stiffening of high damping rubber bearings on the response of base-isolated buildings under near-fault earthquakes", *Mech. Syst. Signal Pr.*, **79**, 297-313. https://doi.org/10.1016/j.ymssp.2016.02.029.

Asher, J.W., Young, R.P. and Ewing, R.D. (1996), "Seismic isolation design of the San Bernardino county medical center replacement project", *Struct. Des. Tall Build.*, **5**(4), 265-279. https://doi.org/10.1002/(SICI)1099-1794(199612)5:4<265::AID-TAL77>3.0.CO;2-X.

Bahnasy, A. and Lavan, O. (2013), "Linear or nonlinear fluid viscous dampers? A seismic point of view", *Structures Congress, ASCE*, Pittsburgh, Pennsylvania, May.

Berkeley (2013), Pacific Earthquake Engineering Research Center (PEER), NGA Database, University of California, Berkeley, http://ngawest2.berkeley.edu.

Cardone, D. and Gesualdi, G. (2014), "Seismic rehabilitation of existing reinforced concrete buildings with seismic isolation: a case study", *Earthq. Spectra*, **30**(4), 1619-1642. https://doi.org/10.1193/110612EQS323M.

Colombo, J.I. and Almazán, J.L. (2017), "Experimental investigation on the seismic isolation for a legged wine storage tank", *J. Constr. Steel Res.*, **133**, 167-180. https://doi.org/10.1016/j.jcsr.2017.02.013.

Constantinou, M.C. and Symans, M.D. (1992), "Experimental and analytical investigation of seismic response of structures with supplemental fluid viscous dampers", Technical Report No. NCEER-92-0032, Department of Civil Engineering, State University of New York, Buffalo.

Deringöl A.H. and Bilgin H. (2018), "Effects of the isolation parameters on the seismic response of steel frames", *Earthq. Struct.*, **15**(3), 319-334. http://dx.doi.org/10.12989/eas.2018.15.3.319.

Goel, R.K. (2004) "Seismic response control of irregular structures using nonlinear dampers", *13th World Conference on Earthquake Engineering*, Vancouver, B.C., Canada, August.

Goel, R.K. (2005), "Seismic response of linear and non-linear asymmetric systems with non-linear fluid viscous dampers", *Earthq. Eng. Struct. Dyn.*, **34**(7), 825-846. https://doi.org/10.1002/eqe.459.

Güler, E. (2013), "Effectiveness of non-linear fluid viscous dampers in seismically isolated buildings against near-field earthquakes", M.Sc. Dissertation, Department of Civil Engineering, Graduate School of Science and Engineering, Istanbul University, Istanbul.

Hall, J.F. and Ryan, K.L. (2000), "Isolated buildings and the 1997 UBC near-source factors", *Earthq. Spectra*, **16**(2), 393-411. https://doi.org/10.1193/1.1586118.

Hall, J.F., Heaton, T.H., Halling, M.W. and Wald, D.J. (1995), "Near-source ground motion and its effects on flexible buildings", *Earthq. Spectra*, **11**(4), 569-605. https://doi.org/10.1193/1.1585828.

He, W.L. and Agrawal, A.K. (2008), "Analytical model of ground motion pulses for the design and assessment of seismic protective systems", *J. Struct. Eng.*, **134**(7), 1177-1188. https://doi.org/10.1061/(ASCE)0733-9445(2008)134:7(1177).

Heaton, T.H., Hall, J.F., Wald, D.J. and Halling, M.W. (1995), "Response of high-rise and base-isolated buildings to a hypothetical M_w 7.0 blind thrust earthquake", *Sci.*, **267**, 206-211. https://doi.org/10.1126/science.267.5195.206.

Hoseini Vaez, S.R., Naderpour, H. and Barros, R.C. (2014), "Influence of equivalent pulses of near fault ground motions on base-isolated RC structures", *Proceedings of the 9th International Conference on Structural Dynamics*, Porto, Portugal, June.

Jensen, H.A. and Kusanovic, D.S. (2014), "On the effect of near-field excitations on the reliability-based performance and design of base-isolated structures", *Prob. Eng. Mech.*, **36**, 28-44. https://doi.org/10.1016/j.probengmech.2014.03.003.

Komodromos, P. (2000), *Seismic Isolation for Earthquake-Resistant Structures*, WIT Press, Southampton, UK.

Losanno, D., Hadad, H.A. and Serino, G. (2017), "Seismic behavior of isolated bridges with additional damping under far-field and near-field ground motion", *Earthq. Struct.*, **13**(2), 119-130. https://doi.org/10.12989/eas.2017.13.2.119.

Martelli, A. (2007), "Seismic isolation and energy dissipation: worldwide application and perspectives", *Earthq. Resist. Eng. Struct.*, **6**, 105-116. https://doi.org/10.2495/ERES070111.
Martelli, A. and Forni, M. (2010), "Seismic isolation and other antiseismic systems recent applications in Italy and worldwide", *Seism. Isolat. Protect. Syst.*, **1**(1), 75-123. https://doi.org/10.2140/siaps.2010.1.75.
Martelli, A. and Forni, M. (2011), "Seismic retrofit of existing buildings by means of seismic isolation: some remarks on the Italian experience and new projects", *Proceedings of the 3rd ECCOMAS Thematic Conference on Computational Methods in Structural Dynamics and Earthquake Engineering*, Corfu, Greece, May.
Martelli, A., Clemente, P., Stefano, A.D., Forni, M. and Salvatori, A. (2014), "Recent development and application of seismic isolation and energy dissipation and conditions for their correct use", *Perspect. Eur. Earthq. Eng. Seismol. Geotech. Geolog. Earthq. Eng.*, **34**, 449-488. https://doi.org/10.1007/978-3-319-07118-3_14.
Martelli, A., Forni, M. and Clemente, P. (2012), "Recent worldwide application of seismic isolation and energy dissipation and conditions for their correct use", *Proceedings of the Fifthteenth World Conference on Earthquake Engineering*, Lisbon, Portugal, September.
Mazza, F. (2018), "Seismic demand of base-isolated irregular structures subjected to pulse-type earthquakes", *Soil Dyn. Earthq. Eng.*, **108**, 111-129. https://doi.org/10.1016/j.soildyn.2017.11.030.
Mazza, F. and Mazza, M. (2017), "Seismic retrofitting by base-isolation of r.c. framed buildings exposed to different fire scenarios", *Earthq. Struct.*, **13**(3), 267-277. https://doi.org/10.12989/eas.2017.13.3.267.
Mazza, F. and Vulcano, A. (2009), "Nonlinear response of RC framed buildings with isolation and supplemental damping at the base subjected to near-fault earthquakes", *J. Earthq. Eng.*, **13**(5), 690-715. https://doi.org/10.1080/13632460802632302.
Mazza, F., Mazza, M. and Vulcano, A. (2017), "Nonlinear response of r.c. framed buildings retrofitted by different base-isolation systems under horizontal and vertical components of near-fault earthquakes", *Earthq. Struct.*, **12**(1), 135-144. https://doi.org/10.12989/eas.2017.12.1.135.
Moeindarbari, H. and Taghikhany, T. (2018) "Seismic reliability assessment of base-isolated structures using artificial neural network: operation failure of sensitive equipment", *Earthq. Struct.*, **14**(5), 425-436. http://dx.doi.org/10.12989/eas.2018.14.5.425.
Naeim, F. and Kelly, J.M. (1999), *Design of Seismic Isolated Structures: from Theory to Practice*, John Wiley & Sons, Inc. California, US.
Nagarajaiah, S. and Ferrell, K. (1999), "Stability of elastomeric seismic isolation bearings", *J. Struct. Eng.*, **125**(9), 946-954. https://doi.org/10.1061/(ASCE)0733-9445(1999)125:9(946).
Nagarajaiah, S., Reinhorn, A.M. and Constantinou, M.C. (1991) "3D-BASIS Nonlinear dynamic analysis of three-dimensional base isolated structures: Part II", Technical Report No. NCEER-91-0005, Department of Civil Engineering, State University of New York, Buffalo.
Narkhade, D.I. and Sinha, R. (2014), "Behavior of nonlinear fluid viscous dampers for control of shock vibrations", *J. Sound Vib.*, **333**(1), 80-98. https://doi.org/10.1016/j.jsv.2013.08.041.
Providakis, C.P. (2008), "Effect of LRB isolators and supplemental viscous dampers on seismic isolated buildings under near-fault excitations", *Eng. Struct.*, **30**(5), 1187-1198. https://doi.org/10.1016/j.engstruct.2007.07.020.
Providakis, C.P. (2009), "Effect of supplemental damping on LRB and FPS seismic isolators under near-fault motions", *Soil Dyn. Earthq. Eng.*, **29**(1), 80-90. https://doi.org/10.1016/j.soildyn.2008.01.012.
Saha, A., Saha, P. and Patro, S.K. (2018), "Seismic protection of the benchmark highway bridge with passive hybrid control system", *Earthq. Struct.*, **15**(3), 227-241. https://doi.org/10.12989/eas.2018.15.3.227.
Saifullah, M.K. and Alhan, C. (2017), "Necessity and adequacy of near-source factors for seismically isolated buildings", *Earthq. Struct.*, **12**(1), 91-108. http://dx.doi.org/10.12989/eas.2017.12.1.091.
SAP2000 (2011), Structural Analysis Program: Static and Dynamic Finite Element Analysis of Structures-Version 15.1, Computers and Structures Inc. (CSI), Berkeley, USA.
Shahi, S.K. and Baker, J.W. (2014), "An efficient algorithm to identify strong-velocity pulses in multicomponent ground motions", *Bull. Seismol. Soc. Am.*, **104**(5), 2456-2466. https://doi.org/10.1785/0120130191.
Somerville, P. (1998), "Development of an improved representation of near-fault ground motions", *SMIP98 Seminar on Utilization of Strong Motion Data*, Oakland, California, September.
Sorace, S. and Terenzi, G. (2001a), "Non-linear dynamic modelling and design procedure of FV spring-dampers for base isolation", *Eng. Struct.*, **23**(12), 1556-1567. https://doi.org/10.1016/S0141-0296(01)00063-3.
Sorace, S. and Terenzi, G. (2001b), "Non-linear dynamic design procedure of FV spring-dampers for base isolation - frame building applications", *Eng. Struct.*, **23**(12), 1568-1576. https://doi.org/10.1016/S0141-0296(01)00064-5.
Sorace, S. and Terenzi, G. (2008), "Analysis and demonstrative application of a base isolation/supplemental damping technology", *Earthq. Spectra*, **24**(3), 775-793. https://doi.org/10.1193/1.2946441.
Sorace, S., Terenzi, G., Bitossi, C. and Mori, E. (2016), "Mutual seismic assessment and isolation of different art objects", *Soil Dyn. Earthq. Eng.*, **85**, 91-102. https://doi.org/10.1016/j.soildyn.2016.03.014.
Tajammolian, H., Khoshnoudian, F., Talaei, S. and Loghman, V. (2014), "The effects of peak ground velocity of near-field ground motions on the seismic responses of base-isolated structures mounted on friction bearings", *Earthq. Struct.*, **7**(6), 1259-1282. http://dx.doi.org/10.12989/eas.2014.7.6.1159.
Tsopelas, P.C., Constantinou, M.C. and Reinhorn, A.M. (1994), "3D-BASIS-ME: Computer program for nonlinear dynamic analysis of seismically isolated single and multiple structures and liquid storage tanks", Technical Report No. NCEER-94-0010; Department of Civil Engineering, State University of New York, Buffalo.
UBC97 (1997), Division IV - Earthquake Regulations for Seismic-Isolated Structures, Uniform Building Code, International Code Council, California, USA.
Uçkan, E., Yenidoğan, C., Tüzün, C. and Erdik, M. (2007), "Seismic isolation applications and current research practice in Turkey", *Proceedings of the Third Structural Engineers World Congress*, Bangalore, India, November.
Warn, G.P. and Ryan, K.L. (2012), "A review of seismic isolation for buildings: historical development and research needs", *Build.*, **2**(3), 300-325. https://doi.org/10.3390/buildings2030300.
Wolff, E.D., Ipek, C., Constantinou, M.C. and Tapan, M. (2015), "Effect of viscous damping devices on the response of seismically isolated structures", *Earthq. Eng. Struct. Dyn.*, **44**(2), 185-198. https://doi.org/10.1002/eqe.2464.

CC